NONLINEAR PERFORMANCE OF CONCRETE BEAM REINFORCED WITH PRESTRESSED HYBRID CFRP/GFRP COMPOSITE SHEET

ZHANG Jian[1], JIA Chao[2*], TIAN Jiawei[1]

[1]Nanjing University of Aeronautics and Astronautics, Nanjing 210016, China
2Shandong University, Jinan 250061, China

[*]Author to whom correspondence should be addressed: E-mail:2410309102@qq.com

Received 20 July 2018; accepted 15 September 2018

ABSTRACT

The consolidation technology of prestressed hybrid fibre CFRP/GFRP sheet takes full advantages of the initiative of the prestressed reinforcement and force transferring of the composite materials features, which belongs to relatively advanced reinforcement strategies in reinforcement area. This paper derives nonlinear composite element and shell element to simulate concrete beam and the prestressed hybrid fibre CFRP/GFRP sheet. Besides, the characters of nonlinear concrete beams are described by the Owen yielding criterion and the Hinton crushing criterion. Meanwhile, the three-dimensional prestressing effects of the composite CFRP/GFRP materials have been realized and the nonlinear finite element computer program of reinforced system has been compiled. In order to determine the best stress condition of prestressed hybrid fibre CFRP/GFRP composite materials, the optimal hybrid CFRP/GFRP ratio is achieved through the systematic calculation based on two main properties which take the strength and ductility properties into consideration. The results show that the optimal CFRP/GFRP hybrid ratio is one of the major factors to impact its mechanical properties of the reinforced structure which has been strengthened by the prestressed hybrid fibre CFRP/GFRP sheet. And the theoretical method and calculation model that determine the optimal hybrid CFRP/GFRP ratio in this paper is reasonable and reliable. The research conclusions can be used as a reference in practice construction design.

Key words: the optimal hybrid ratio; concrete beam; hybrid composite CFRP/GFRP sheet; finite element

1. INTRODUCTION

The reinforced technology by using FRP sheet has a certain application in practical engineering, it basically adopts the passive paste of non prestressed FRP sheet to raise the bearing capacity of components. The weight of bridge is often a significant proportion of the total load, and passive paste FRP is only used for resistance, the influence of the application effect on flexural member is not satisfactory[1-3]. Therefore, strengthening with prestressed FRP sheet paste is better than that of non-prestressed FRP sheet paste method. In order to improve the effectiveness of reinforcement, the FRP sheet is stressed by using the appropriate tension machine and then paste on the structure. This kind of reinforcement technology can make use of FRP material more effectively and solve the above problems in all aspects[4-6]. Compared with the study of non-prestressed FRP sheet, the study of prestressed FRP sheet only appears in recent years. Like traditional prestressed structure, the initial prestress can be used to balance structure of self-respect and part of the load, delay the development of the cracks, reduce the width of the crack and deflection of structure, alleviate stress of the steel, and improve the ultimate bearing capacity of concrete beams [7-10]. Two fibres hybridized together can show better mechanical properties than a single fibre, and their properties are not a simple superposition of single materials[11-15]. The reasons are as follows. When using two kinds of fibres are blended, high extensibility fibre can afford additional load which is caused by low extensibility fibre fracture and increase the average fracture strain of the hybrid fibres[16]. Using two kinds of blended fibres can delay the failure process. And the fibres which have lower ductility and are easier to crack still can be in the form of short fibres with high ductility fibres to work together until all fibre fracture in succession[17]. In order to meet the specific needs in different projects, the ratio of the fibres can be adjusted to improve the reinforced performance. There are some other structures which are reinforced with fibres or with CFRP/GFRP [18]. The different kinds of solid-rebar combinative element and solid-beam combinative element are fabricated to accomplish the elastic analysis for the concrete cable stayed bridge, the PC box girder bridge and RC rectangle beam. Among the available achievements, the majority can only be applied to structural elastic analysis due to the complexity of the

3-dimensional nonlinear combinative element[19]. The layer element is creatively explored to simulate common steels and prestressed steels, then nonlinear structural analysis is completed. Results show that due to the crossing and overlapping particularity between the common steel layer and the prestressed steel layer, it is hardly possible to precisely realize the spacial prestress effect by layer element[20]. As for improvement, the total Lagrange rebar element is developed to imitate prestressed CFRP rebar, then a new combinative element is engendered to put the nonlinear mechanical analysis of the concrete beam with prestressed CFRP rebars into practice. Actually, the total Lagrange rebar element can only depict the axial tensile or compressive performance of the prestressed CFRP rebar unfortunately, it cannot embody the fundamental bending or shearing performance[21]. Comparatively, the beam element can comprehensively reflect the reinforcement action of the prestressed CFRP rebars to the concrete structures.

This paper establishes a nonlinear mechanics model of concrete beam reinforced with prestressed CFRP/GFRP fibre to calculate the reinforced structure, and the optimal hybrid CFRP/GFRP ratio is achieved through the systematic calculation based on two main properties which take the strength and ductility properties into consideration.

2. MECHANICAL MODEL OF CONCRETE BEAM REINFORCED WITH HYBRID PRESTRESSED CFRP/GFRP SHEET

In the past achievements of a single FRP or hybrid FRP reinforced concrete beam[10-12], most are focused on the experimental study of the specimens. Because of the high nonlinear performance of hybrid fibre reinforced concrete beam element and the complexity of three dimensional nonlinear programming, the theoretical calculation and analysis is done by using the commercial finite element software[22-24]. Commercial finite element software is relatively mature in the elastic analysis, but it has some problems which have to be solved before used in the nonlinear analysis on the material constitutive numerical stability and convergence[25-27]. In this paper, the concrete beam with prestressed CFRP/GFRP fibre sheet is analyzed by nonlinear combination element and shell element simulation.

The degraded shell element as shown in Fig.1 has 9 nodes, among which the 4 corner nodes are the controlling nodes. And the spatial geometric positions of the other 5 nodes can be determined by the 4 controlling nodes. Each node of the degraded shell element has three independent degrees of freedom of linear displacement and two independent degrees of freedom of angular displacement. The rotation variable is not restricted by the slope of the middle plane and the transverse shearing deformation is allowed. ξ, η, ζ in Fig.1 are the natural curve coordinate system and $\bar{\mathbf{v}}_{1k}, \bar{\mathbf{v}}_{2k}, \bar{\mathbf{v}}_{3k}$ are the nodal coordinate system of node k in degraded shell element. Δ_{1k} and Δ_{2k} are respectively the linear displacement along the nodal coordinate system $\bar{\mathbf{v}}_{1k}$ and $\bar{\mathbf{v}}_{2k}$. β_{1k}, β_{2k} are respectively the angular displacement rotated by $\bar{\mathbf{v}}_{2k}$ and $\bar{\mathbf{v}}_{1k}$. u_k, v_k, w_k are the linear displacements of node k in the global coordinate system. The midsection has 9 controlling nodes as shown in Fig.2, which is used to describe the degradation element of information about the corresponding element decreased significantly.

The displacement of 9 nodes degradation element is as follows:

$$\boldsymbol{\delta}_i = [u_i \quad v_i \quad w_i \quad \beta_{1i} \quad \beta_{2i}]^T \tag{1}$$

In this formula, $[u_i \; v_i \; w_i]$ is the line displacement of the node i in the overall system, $[\beta_{1i} \; \beta_{2i}]$ is the angle displacement of the i node in the node coordinates. Displacement field by interpolation can be expressed by the shape function:

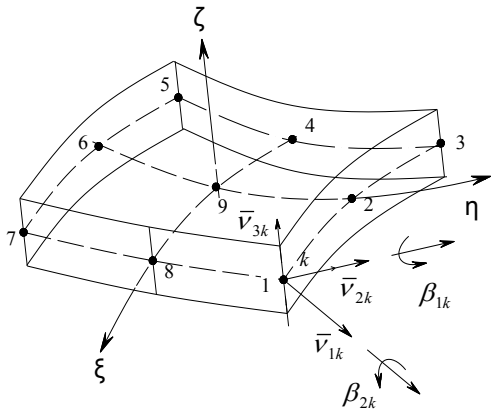

Fig.1: The degraded shell element

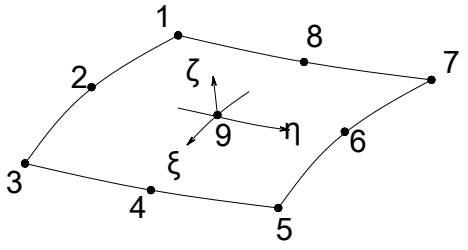

Fig.2: Local coordinate of the midsurface

$$u=\sum_{i=1}^{n}N_i u_i+\sum_{i=1}^{n}N_i\frac{h_i}{2}\zeta(v_{1i}^{x}\beta_{1i}-v_{2i}^{x}\beta_{2i}) \quad (2)$$

$$v=\sum_{i=1}^{n}N_i v_i+\sum_{i=1}^{n}N_i\frac{h_i}{2}\zeta(v_{1i}^{y}\beta_{1i}-v_{2i}^{y}\beta_{2i}) \quad (3)$$

$$w=\sum_{i=1}^{n}N_i w_i+\sum_{i=1}^{n}N_i\frac{h_i}{2}\zeta(v_{1i}^{z}\beta_{1i}-v_{2i}^{z}\beta_{2i}) \quad (4)$$

Where N_i is the shape function of node i, h_i is the element thickness of node i, v^{x}_{1i} is a cosine between the node coordinate v_1 and the overall system x of node i (the same to others).

Concrete, stirrups and structural reinforcement in the concrete beams can take concrete layer element to simulate as shown in Fig.3. The CFRP/GFRP fibre sheet which uses the shell element is shown in Fig.4. For vertical reinforced (main), using layer element simulating is too approximate, this paper uses composition element to simulate concrete beams. As shown in Fig.3, the main reinforcement in the combination element in concrete beams starts with point A and ends with point B. By using the displacement interpolation Eqs.(2) to (4), the node displacement in main reinforcement elements can be expressed as:

$$\begin{bmatrix}u_A\\v_A\\w_A\\u_B\\v_B\\w_B\end{bmatrix}=\sum_{i=1}^{n}\begin{bmatrix}N_i^A & & & N_i^A\frac{h_i}{2}\zeta_A v_{1i}^{x} & -N_i^A\frac{h_i}{2}\zeta_A v_{2i}^{x}\\ & N_i^A & & N_i^A\frac{h_i}{2}\zeta_A v_{1i}^{y} & -N_i^A\frac{h_i}{2}\zeta_A v_{2i}^{y}\\ & & N_i^A & N_i^A\frac{h_i}{2}\zeta_A v_{1i}^{z} & -N_i^A\frac{h_i}{2}\zeta_A v_{2i}^{z}\\ N_i^B & & & N_i^B\frac{h_i}{2}\zeta_B v_{1i}^{x} & -N_i^B\frac{h_i}{2}\zeta_B v_{2i}^{x}\\ & N_i^B & & N_i^B\frac{h_i}{2}\zeta_B v_{1i}^{y} & -N_i^B\frac{h_i}{2}\zeta_B v_{2i}^{y}\\ & & N_i^B & N_i^B\frac{h_i}{2}\zeta_B v_{1i}^{z} & -N_i^B\frac{h_i}{2}\zeta_B v_{2i}^{z}\end{bmatrix}\begin{bmatrix}u_i\\v_i\\w_i\\\beta_{1i}\\\beta_{2i}\end{bmatrix}=\sum_{i=1}^{n}\mathbf{R}_i\boldsymbol{\delta}_i \quad (5)$$

Where N^A_i is the value of node A about the main reinforcement element in the shape function, N^A_i is the value of node B; ζ_A is the value of element's starting point A in the local ζ coordinates, ζ_B is the value of element's end point B in the local ζ coordinates, δ_i is the array of shell element node displacement , R_i is the transformation matrix. Take $\delta s=[u_A\ v_A\ w_A\ u_B\ v_B\ w_B]^T$, $R=[R_1\ R_2....R_n]$, $\delta c=[\delta_1{}^T\ \delta_2{}^T....\delta^T_n]^T$, then Eq.(5) is written as:

$$\delta_s=R\delta_c \quad (6)$$

Application of virtual work principle, the contribution of the main reinforcement element can be put into the stiffness matrix of the composition element:

$$\mathbf{K}_S=\mathbf{R}^T\overline{\mathbf{K}}_S\mathbf{R} \quad (7)$$

Where K_S is the element's contribution to the composition element stiffness matrix; $\overline{\mathbf{K}}_S$ is advocate muscle stiffness matrix of the overall coordinate system. The contribution of concrete layer, stirrups and structural reinforcement layer to stiffness matrix can use Gaussian formula to calculate which has been validated in Ref.[12]. Hybrid reinforcement of structure with CFRP/GFRP fibre sheet thickness is small, and single layer thickness is between 0.15 mm to 0.5 mm. The initial stress equivalent load method is adopted to realize the space prestressing effect of CFRP/GFRP sheet. Because of adopting advanced steel plate bolt anchorage technique and paste for prestressed CFRP/GFRP sheet, the failure mode of test reinforcement beam is broken in the form of fibre blah or rib fracture, and the failure mode of fibre sheet strip damage does not happen in this paper. Therefore, this article does not consider the interface bond-slip effect, and the hybrid fibre sheet element with concrete beam element uses the node processing.

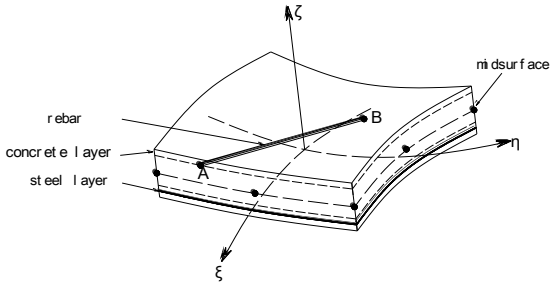

Fig.3: Combined shell element with rebar

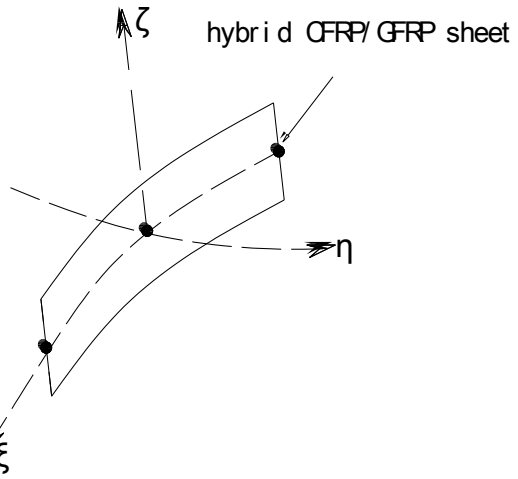

Fig.4: Hybrid CFRP/GFRP sheet of the derived element

2 CRITERION FOR THE CONCRETE BEAM REINFORCED WITH PRESTRESSED CFRP /GFRP FIBRE SHEET

2.1 Concrete material model

2.1.1 Yielding model

The Owen triaxial yielding criterion is utilized as:

$$f(I_1,J_2)=\left(\alpha I_1+3\beta J_2\right)^{1/2}=\sigma_0 \tag{8}$$

Where I_1 is the first invariant stress tensor, J_2 is the secend invariant stress tensor, σ_0 is equivalent stress, f_c is the concrete compressive strength, α and β are the material parameters which are respectively determined according to the uniaxial compression and biaxial compressive test calibration.

$$\alpha=\frac{1-t^2}{2t-t^2}\sigma_0,\ \beta=\frac{2t-1}{2t-t^2} \tag{9}$$

Where $t=f_{cc}/f_c$, f_{cc}, is bidirectional compressive strength.

2.1.2 Hardening model

Hardening model determine the subsequent yield surface movement in the process of plastic deformation. It determines the loading surface and the relationship between the cumulative plastic strains. The effective stress and effective plastic strain can be used to describe the mechanical behavior of uniaxial test about concrete to uniaxial test[28-29]. The parameters H' of the elastic-plastic matrix can be represented by a slope of effective stress on the effective plastic strain ε_p, the expression shows as follows:

$$H'=\frac{d\sigma}{d\varepsilon_p} \tag{10}$$

The expression of the relation between uniaxial effective stress σ and effective plastic strain ε_p based on the Madrid parabolic is shown as follows:

$$\sigma=E_0(\varepsilon_e+\varepsilon_p)-\frac{1}{2}\frac{E_0}{\varepsilon_0}(\varepsilon_e+\varepsilon_p)^2 \tag{11}$$

Where E_0 is the initial elastic modulus, ε_0 is the total strain at the uniaxial compressive strength f_c and its value is $2f_c/E_0$. ε_e is the elastic strain, and its value is σ/E_0. The expression can be determined by uniaxial effective stress and effective plastic strain equation:

$$\sigma=-E_0\varepsilon_p+\sqrt{2E_0^2\varepsilon_0\varepsilon_p}\qquad(0.3f_c<\sigma\le f_c) \tag{12}$$

Thus the parameter H' can be solved using Eqs. (9) and (11).

2.1.3 Crushing model

Concrete crush is controlled by strain, and the expression of Hinton crush model is shown as follows:

$$F(I_1',J_2')=\left(\alpha I_1'+3\beta J_2'\right)^{1/2}=\varepsilon_u \tag{13}$$

Where I'_1 is the first invariant strain tensor, J'_2 is the second invariant of deviator strain, ε_u is the ultimate compressive strain of concrete. α and β are the parameters used in Eq.(9).

2.2 CFRP/GFRP materials model

It is assumed that the CFRP/GFRP fibre sheet and concrete have good bonding strength. And CFRP/GFRP fibre sheet is anisotropic and cannot bear the pressure and bending moment of the material, and it can only bear the longitudinal strain. Thus the CFRP/GFRP fibre sheet is perfectly elastic before breaking. According to the test, the ultimate strength of CFRP/GFRP fibre sheet is 2956.3MPa. The CFRP/GFRP fibre sheet will completely fail when the strength of CFRP/GFRP fibre sheet gets 2956.3MPa.

3. NONLINEAR CONVERGENCE CRITERIA

This paper uses both the equivalent stiffness method and the tangent stiffness method. The tangent stiffness method is utilized in the first iteration in the each incremental step, and the equivalent stiffness method is used in the iterative calculation of the rest of the incremental steps. Thus the displacement convergence criterion is adopted:

$$\frac{\left\|\boldsymbol{\delta}_{i+1}-\boldsymbol{\delta}_i\right\|_2}{\left\|\boldsymbol{\delta}_{i+1}\right\|_2}<\varepsilon \tag{14}$$

Where is the convergent solution of the incremental step i of the solution of nonlinear equations which is the value of the whole displacement vector of the CFRP/GFRP fibre reinforced concrete beam in step increment i. δ_{i+1} is the convergent solution of the incremental step i+1 of the solution of nonlinear equations. The value 2.5% is used as the convergence tolerance ε in Eq.(14).

4. THE OPTIMAL HYBRID PROGRAM DEVELOPED AND CALCULATION ANALYSIS

4.1 Basic parameters of computational concrete beam

The size of prestressed CFRP/GFRP fibre reinforced concrete beam is 150mm×250 mm×2800 mm; longitudinal reinforcement is 2φ14; stirrup isφ8@150 symmetrical reinforcement; the thickness of protective layer is 25 mm. The thickness of fibre sheet

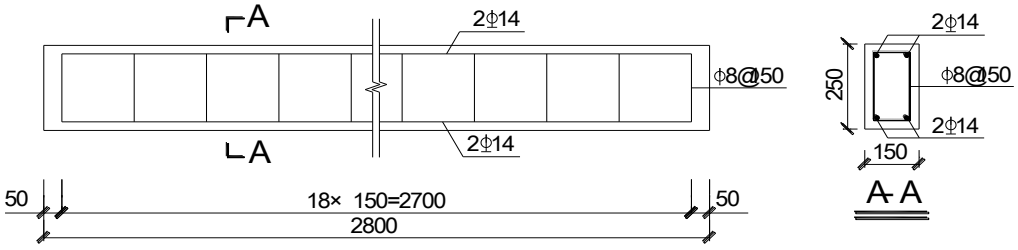

Fig.5: Dimensions of the studied concrete beam/mm

Table 1: Performance of hybrid CFRP/GFRP fibre with different ratio

Kind of FRP	Symbol	Tensile Strength(MPa)	Tensile Modulus(MPa)	Ductility (%)
CFRP	C	3848.2	234200	1.64
CFRP-GFRP 1:1	CG11	2838.83	171260	2.03
CFRP-GFRP 1:2	CG12	2349.73	124088	2.29
CFRP-GFRP 1:3	CG13	2161.12	90012	2.46
CFRP-GFRP 2:1	CG21	3063.48	190963	1.85
CFRP-GFRP 3:1	CG31	3266.34	207213	1.70
GFRP	G	2003.21	75021	2.71

is 0.23mm. Section size and reinforcement of test beam are shown in Fig.5. Based on the different ratio of CFRP/GFRP hybrid fibre performance by composite material production elements and after comprehensive comparison, seven kinds of hybrid fibre are chosen in theoretical analysis as shown in table 1 to find the optimal mixture ratio, which is based on both strength and ductility index calculation analysis of prestressed CFRP/GFRP fibre sheet. For convenient, carbon fibre can be abbreviated to C, carbon-glass 1:1 can be abbreviated to CG11, carbon-glass 1:2 can be abbreviated to CG12, carbon-glass 1:3 can be abbreviated to CG13, carbon-glass 2:1 can be abbreviated to CG21, carbon-glass 3:1 can be abbreviated to CG31, glass fibre can be abbreviated to G.

4.2 The finite element model

Nonlinear combination element and shell element are adopted to establish the calculation model of CFRP/GFRP fibre reinforced concrete beam. The model has 120 elements and 533 nodes, and the prestressed CFRP/GFRP fibre sheet shell element is 20; the rest is the concrete beam element; the finite element model is shown in Fig.6. Each load point is loaded as 3kN in the whole process of analysis. When the load step is increased, the added load is corresponding increased at the rate of 3kN per load step.

4.3 The finite element results

The optimal mixture ratio is studied in the whole process of calculation about prestressed CFRP/GFRP fibre reinforced concrete beams in Fig.7, the concrete strength level is C25, and the fibre sheet prestressed degree is 0-0.4. The crack load and yield load, ultimate load and the load level at the time of the prestressed CFRP/GFRP fibre sheet, midspan deflection of beam body development data can be extracted through the process. Reinforcement effect and the optimal mixture ratio are defined by strength and ductility index evaluation in Table 2.

The results from simulation are shown in Fig. 7, including the load rating, the load deflection curves of different fibre sheet reinforced concrete beam and the development curve of stress of fibre sheet change in rule. At the beginning of loading, deflection and fibre stress develop more gently; however when reached yield load, the mid span deflection and fibre stress develop rapidly until the structure damage. These conclusions are consistent with existing conclusions, and theoretical analysis model in this paper is established correctly. The strength and

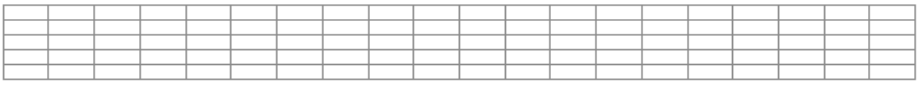

Fig.6: The analytical finite element model

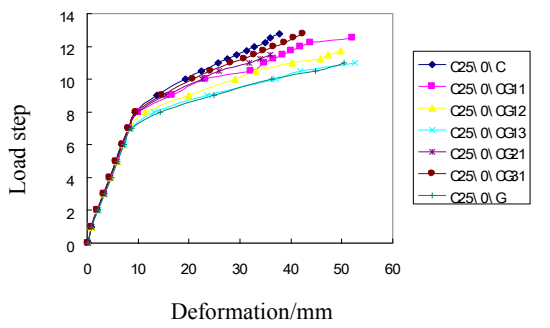

a. Load-deformation curvation when prestress degree is 0

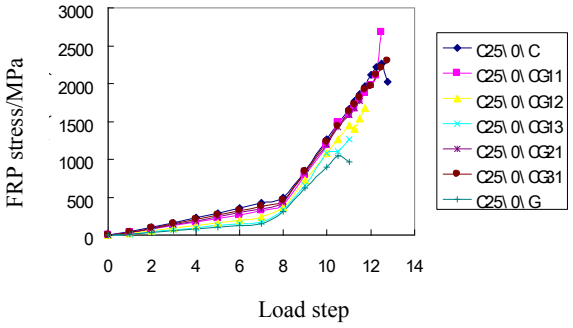

b. Load-FRP stress curvation when prestress degree is 0

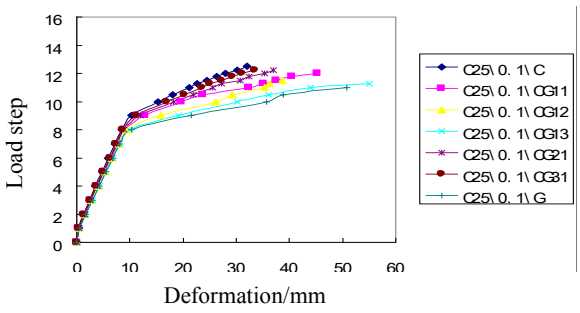

c. Load-deformation curvation when prestress degree is 0.1

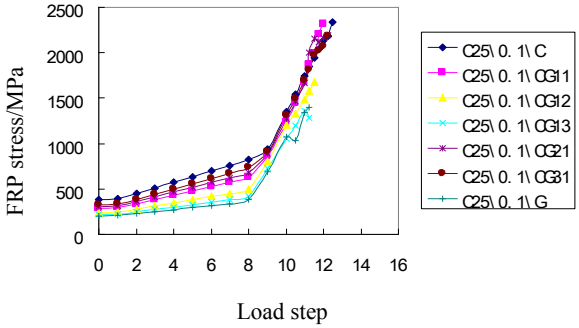

d. Load-FRP stress curvation when prestress degree is 0.1

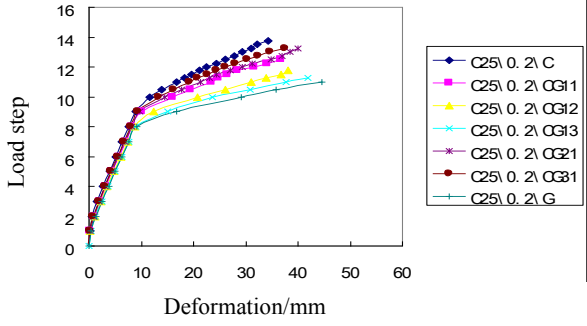

e. Load-deformation curvation when prestress degree is 0.2

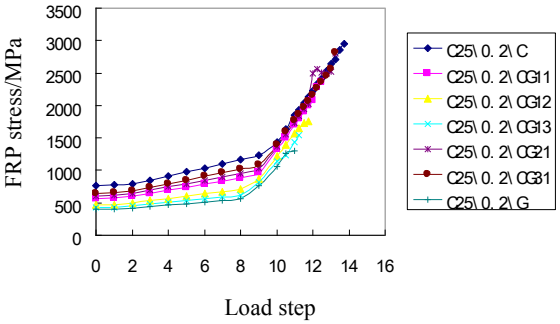

f. Load-FRP stress curvation when prestress degree is 0.2

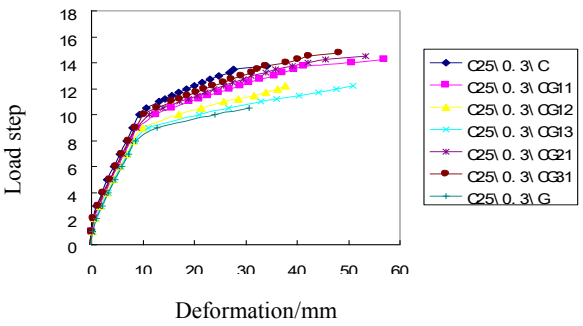

g. Load-deformation curvation when prestress degree is 0.3

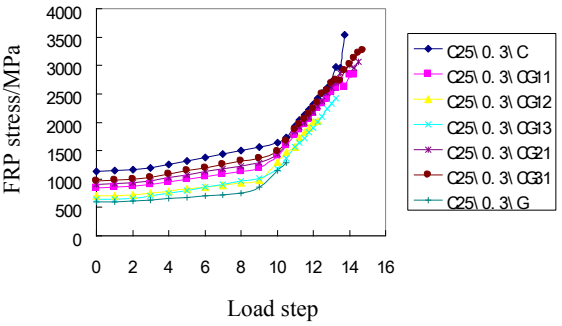

h. Load-FRP stress curvation when prestress degree is 0.3

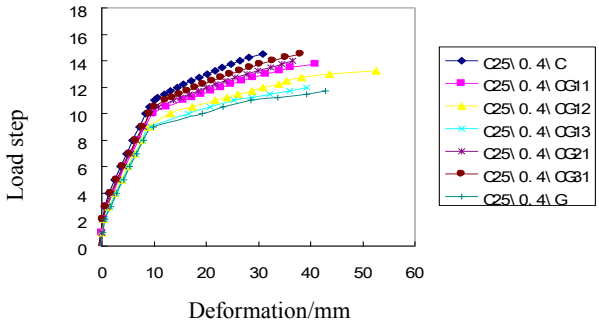

i. Load-deformation curvation when prestress degree is 0.4

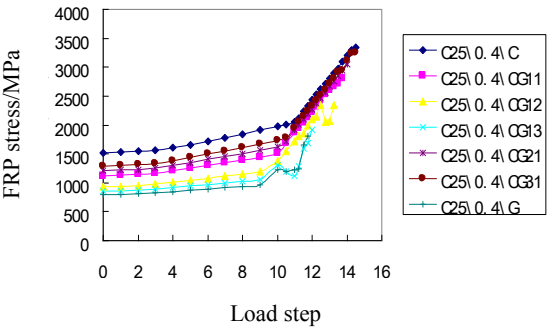

j. Load-FRP stress curvation when prestress degree is 0.4

Fig.7: Computational results of concrete beams reinforced with prestressed hybrid CFRP/GFRP sheet

Table 2: Typical load, deflection and ductility characteristics of RC beams strengthened with prestressed CFRP/GFRP sheet

Prestress degree	Kind of FRP sheet	Crack load/kN	Crack deformation/ mm	Yield load/kN	Yield deformation/ mm	Ultimate load/kN	Ultimate deformation/ mm	Ductility
0	C	6.00	0.82	48.00	9.45	76.50	37.70	3.99
	CG11	6.00	0.83	48.00	10.12	75.00	52.10	5.15
	CG12	6.00	0.84	42.00	8.47	70.50	49.70	5.86
	CG13	6.00	0.85	42.00	8.63	66.00	52.62	6.10
	CG21	6.00	0.83	48.00	9.88	69.00	35.97	3.64
	CG31	6.00	0.82	48.00	9.58	76.50	42.37	4.42
	G	6.00	0.86	42.00	8.70	66.00	50.46	5.80
0.2	C	12.00	0.62	54.00	8.91	82.50	34.26	3.84
	CG11	12.00	0.94	54.00	10.00	75.00	36.72	3.67
	CG12	12.00	1.10	48.00	8.72	70.50	38.02	4.36
	CG13	12.00	1.20	48.00	9.00	67.50	41.94	4.66
	CG21	12.00	0.86	54.00	9.62	79.50	39.92	4.15
	CG31	12.00	0.78	54.00	9.35	79.50	37.48	4.01
	G	12.00	1.27	48.00	9.17	66.00	44.55	4.86
0.4	C	24.00	1.38	63.00	9.17	87.00	30.95	3.37
	CG11	18.00	1.04	60.00	9.95	82.50	40.88	4.11
	CG12	18.00	1.36	54.00	8.99	79.50	52.58	5.85
	CG13	12.00	0.53	54.00	9.39	72.00	39.27	4.18
	CG21	18.00	0.90	60.00	9.42	84.00	36.54	3.88
	CG31	18.00	0.81	60.00	9.11	87.00	38.10	4.18
	G	12.00	0.61	54.00	9.84	70.50	42.84	4.35

ductility index evaluation CFRP/GFRP optimal mix ratio, extraction cracking load, yield load and ultimate load are listed in Table 2. By comparing different hybrid ratio, the strength index and ductility indexes of beams strengthened with CG11 are both elevated, thus CG11 is the optimal hybrid form.

5. CONCLUSIONS

Reinforced concrete beams are studied in the whole process, which are reinforced by carbon fibre, carbon-glass 1:1, carbon-glass 1:2, carbon-glass 1:3, carbon-glass 2:1, carbon-glass 3:1 and glass fibre. Characteristics of prestressed GFRP reinforcement values are relatively low, thus prestressed GFRP reinforcement is not appropriate. Characteristic value of load strengthened with prestressed CFRP sheets was improved compared with the hybrid fibre cracking load, which increase a little while the residual strength caused by the excessive waste and the ductility index both decline. Therefore, the hybrid with CFRP and GFRP sheet can fully realize their respective advantages. By comparison of different hybrid ratio, the strength index and ductility indexes of beams strengthened with CG11 are both elevated, thus CG11 is the optimal hybrid form.

ACKNOWLEDGEMENTS

Project supported by National Natural Science Foundation of China(No. 11232007), Natural Science Foundation of Jiangsu Province(No. BK20130787), the Fundamental Research Funds for the Central Universities (No. NS2014003), Research Fund of Zhejiang Guangchuan Engineering Consulting Co., Ltd(No. Y1704), Research Fund of Graduate Education and Teaching Reform of NUAA(No. 2017-2), Research Fund of Education and Teaching Reform of College of Aerospace Engineering, NUAA(No. 2017-5).

References:

[1] X. J. Wei, J. J. Zhang and S. M. Zhang: 'Group for shield tunnel construction induced ground maximal settlement'. Rock Soil Mech., 2008, 29, 445-448.

[2] J. Zhang, J. S.Ye and C. W. Zhou: 'Powell's optimal identification of material constants of thin-walled box girders based on Fibonacci series search method'. Applied Math. Mech., 2011, 32, 97-106.

[3] J. Zhang, C. W. Zhou, W. G. Lan, et al: 'Nonlinear

dynamical identification of displacement parameters of multi-cell curve box based on Markov error theory', Chinese J. Applied Mech., 2010, 27, 746-750.

[4] M. S. Khaled and B. K. John: 'Literature review in analysis of box-girder bridges'. J. Bridge Eng., 2002, 7, 134–143.

[5] K. Babu and M. Devdas: 'Correction of errors in simplified transverse bending analysis of concrete box-girder bridges', J. Bridge Eng., 2005, 10, 650-657.

[6] R. A. Ghani, U. Hangang: 'Thin-walled multicell straight box-girder finite element', J. Struct. Eng., 1991, 117, 2953-2971.

[7] Q. Z. Luo, Q. S. Li and J. Tang: 'Shear lag in box girder bridges', J. Bridge Eng., 2002, 7, 308–313.

[8] J. Zhang, J. S. Ye and C. Q. Wang: 'Dynamic Bayesian estimation of displacement parameters of continuous thin-walled straight box with segregating slab based on CG method', Chinese J. Comp. Mech., 2008, 25, 574-580.

[9] J. Zhang, W. G. Lan and J. Lin: 'Theoretical model of revised Powell back analysis of composite T-beam with error function', Adv. Mater. Res., 2011, 146-147, 1519-1523.

[10] J. Zhang, W. G. Lan and B. Yu: 'Stochastic Gaussian optimized inversion of mechanical parameters of reinforced concrete single T-shaped beam', Adv. Mater. Res., 2011, 163-164, 1874-1878.

[11] T. Ohkami and Y. Ichikawa: 'A boundary element method for identifying orthotropic material parameters', Num. Analy. Method Geom., 1991, 15,609-625.

[12] J. Zhang, C. W. Zhou, X. Lei, et al: 'Nonlinear beam-shell composite element of HPC beam mixed with CFRP/GFRP rebars', Acta Mater. Comp. Sin., 2010, 27, 139-146.

[13] David, W., 2005. Pipeline supported on a non-uniform Winkler soil model. Journal of Geotechnical and Geoenvironmental Engineering, 131(10): 1301-1304.

[14] Zidi, M., Tounsi, A., Houari, M.S.A., et al., 2014. Bending analysis of FGM plates under hygro-thermo-mechanical loading using a four variable refined plate theory. Aerospace Science and Technology, 34: 24-34.

[15] Meziane, M.A.A., Abdelaziz, H.H., Tounsi, A., 2014. An efficient and simple refined theory for buckling and free vibration of exponentially graded sandwich plates under various boundary conditions, Journal of Sandwich Structures and Materials, 16(3), 293-318.

[16] Roberto, F.A., Alexandre, B.P., Jorge, G.Z., 2002. Numerical analysis of a tunnel in residual soils. Journal of Geotechnical and Geoenvironmental Engineering, 128(3): 227-236.

[17] Bousahla, A.A., Houari M.S.A., Tounsi A., et al., 2014. A novel higher order shear and normal deformation theory based on neutral surface position for bending analysis of advanced composite plates. International Journal of Computational Methods, 11(6), 19-30

[18] Wen, Q.J., 2011. Long-term effect analysis of prestressed concrete box-girder bridge widening. Construction and Building Materials, 25(4): 1580-1586.

[19] Khader, M.H., Zhuang, X.Y., He P.F., et al., 2016. Fracture toughness of polymeric particle nanocomposites: Evaluation of models performance using Bayesian method. Composite Science and Technology, 126(4):122-129.

[20] Nanthakumar, S.S., Lahmer, T., Zhuang, X., et al., 2016. Detection of material interfaces using a regularized level set method in piezoelectric structures. Inverse Problems in Science and Engineering, 24(1), 153-176.

[21] Bennoun, M., Houari, M.S.A., Tounsi, A., 2016. A novel five variable refined plate theory for vibration analysis of functionally graded sandwich plates. Mechanics of Advanced Materials and Structures, 23(4), 423-431.

[22] Hamidi, A., Houari, M.S.A., Mahmoud, S.R., et al., 2015. A sinusoidal plate theory with 5-unknowns and stretching effect for thermomechanical bending of functionally graded sandwich plates. Steel and Composite Structures, 18(1), 235-253.

[23] Bourada, M., Kaci, A., Houari, M.S.A., et al., 2015. A new simple shear and normal deformations theory for functionally graded beams. Steel and Composite Structures, 18(2), 409-423.

[24] Vu-Bac, N., Lahmer, T., Zhuang, X, et al., 2016. A software framework for probabilistic sensitivity analysis for computationally expensive models. Advances in Engineering Software, 100: 19-31.

[25] Beldjelili, Y., Tounsi, A., Mahmoud, S.R., 2016. Hygro-thermo-mechanical bending of S-FGM plates resting on variable elastic foundations using a four-variable trigonometric plate theory, Smart Structures and Systems, 18(4), 755-786.

[26] Yahia, S. A., Atmane, H.A., Houari, M.S.A., et al., 2015. Wave propagation in functionally graded plates with porosities using various higher-order shear deformation plate theories. Structural Engineering and Mechanics, 53(6), 1143-1165.

[27] Zhang, J., Zhou, C.W., Jia, C., et al., 2017. Powell inversion mechanical model of foundation parameters with generalized Bayesian theory, Journal of Zhejiang University-SCIENCE A(Applied Physics & Engineering), 18(7), 567-578.

[28] Besseghier, A., Houari, M.S.A., Tounsi, A., et al., 2017. Free vibration analysis of embedded nanosize FG plates using a new nonlocal trigonometric shear deformation theory, Smart Structures and Systems, 19(6), 601-614.

[29] Hamdia, K.M., Silani. M., Zhuang, X.Y., et al., 2017. Stochastic analysis of the fracture toughness of polymericnanoparticle composites using polynomial chaos expansions, International Journal of Fracture, 206: 215-227.